Thermographic Particle Velocimetry (TPV): An Experimental Technique for Simultaneous Interfacial Temperature and Velocity Measurements Using an Infrared Thermograph

A. Charogiannis[1], I. Zadrazil[1], C. N. Markides[1*]
1: Clean Energy Processes (CEP) Laboratory, Department of Chemical Engineering, Imperial College London, London SW7 2AZ, United Kingdom
* Correspondent author: c.markides@imperial.ac.uk

Keywords: Infrared thermography (IR), Particle image velocimetry (PIV), Thermographic particle velocimetry (TPV), Film flows

ABSTRACT

We present an experimental measurement technique that is capable of recovering two-dimensional (2-D) surface temperature and velocity measurements at the interface of multiphase flows by employment of a single infrared (IR) imager. The technique exploits the emissivity disparity (in the IR) between the fluid and highly-reflective particles; when suspended near or at the interface, these particles are distinguished from the surrounding fluid due to their differing emissivity without the requirement for a light source (laser or flash-lamp). Despite the fact that the development of this technique, which we refer to as "thermographic particle velocimetry" (TPV), builds upon our previous work on heated falling-film flows by application of planar laser induced fluorescence (PLIF) and IR imaging, the same measurement principle can also be applied for the recovery of 2-D temperature- and velocity-field information at the common interface of any flow with a significant density gradient between two fluid-phases.

A series of image processing steps are necessary in order to recover accurate temperature and velocity data, such as the decomposition of raw images into thermal and particle images, the application of filtering operations, perspective distortion corrections and spatial calibrations, and the implementation of standard PIV algorithms. These steps are demonstrated by application of the TPV methodology in a heated and stirred flow in an open container. The efficacy of TPV in recovering 2-D surface temperature and velocity data is examined by carrying out dedicated validation experiments for the measurement of interfacial temperature and velocity. The obtained deviations between the results generated using conventional techniques and those from TPV do not exceed the errors associated with the former. The proposed technique is also demonstrated by simultaneously recovering temperature and velocity data from the gas-liquid interface of wavy film-flows downstream of a localized heater.

1. Introduction

Ever since the Kapitza brothers (Kapitza 1948, Kapitza and Kapitza 1949) conducted their pioneering work on falling liquid-films, numerous experimental investigations have been devoted to the study of this particular class of interfacial flows (Alekseenko, Nakoryakov and Pokusaev 1985, Moran, Inumaru and Kawaji 2002). Efforts are still ongoing, motivated by the

desire to harness the excellent heat and mass transfer capabilities of falling liquid-films in the wide range of engineering and industrial applications in which they are employed. Examples of such applications include cooling schemes used in electronic and mechanical systems, heat exchangers, film condensers, evaporators and reactors, to name but a few.

Optical techniques have been developed and are extensively employed in a variety of contemporary experimental investigations in the fields of fluid mechanics and transport processes, forming an inherent part of the aforementioned research efforts. For example, planar laser-induced fluorescence (PLIF) which involves the illumination and imaging of a planar section through the flow of interest, has been employed by many researchers as it allows for spatiotemporally resolved velocity, in conjunction with the use of an appropriate velocimetry technique (Morgan, Markides, Hale et al. 2012, Morgan, Markides, Zadrazil et al. 2013, Zadrazil and Markides 2014, Zadrazil, Matar and Markides 2014, Charogiannis, An and Markides 2015), or temperature information to be recovered simultaneously with the film-height (Mathie and Markides 2013, Mathie, Nakamura and Markides 2013, Markides, Mathie and Charogiannis 2015). Optical velocimetry techniques can be grouped into two broad categories depending on whether particle seeding or molecular tagging is employed. Particle image velocimetry (PIV) and particle tracking velocimetry (PTV) belong to the former category, and allow for 2-D or 3-D flow-field characterization by sequential illumination and imaging of the scattered or fluorescence signal from the particles seeded in the flow. In turn, these allow for tracking of the motion of particle groups (PIV) or individual particles (PTV), typically using a multi-pass cross-correlation approach during post-processing.

In addition to laser-based measurement tactics, infrared (IR) thermography has been employed in a large number of heated film-flow investigations, contributing significantly to our understanding of the effects of the applied heat flux on film topology and the associated heat transfer processes. In more detail, IR thermography has been employed in order to elucidate the link between the applied heat flux and the formation and spatiotemporal evolution of film regions dominated by thermal rivulets (Chinnov and Kabov 2007, Chinnov and Shatskii 2010, Chinnov, Shatskii and Kabov 2012, Chinnov and Abdurakipov 2013), investigate film contraction/expansion as a function of both flow and heating parameters (Zhang, Zhao, Geng et al. 2007, Zhang, Peng, Geng et al. 2009, Peng, Wang, Geng et al. 2012), and finally in order to understand the interaction between thermocapillary forces and the hydrodynamics of regular wave-patterns (Kabov, Scheid, Sharina et al. 2002, Lel, Kellermann, Dietze et al. 2008, Rietz, Rohlfs, Kneer et al. 2015). It should finally be noted that the experimental techniques and publications cited here are by no means exhaustive, but rather only indicative of the number of intriguing studies carried out by employment of optical diagnostics in film flows.

2. Experimental methodology

In this contribution we propose an alternative approach to the use of basic IR imaging for the study of heated falling-film flows. Building upon our recent work with unsteady and conjugate heat transfer in thin liquid-film flows (Mathie, Nakamura and Markides 2013, Markides, Mathie and Charogiannis 2015), and the experimental investigation of the hydrodynamic characteristics of isothermal films by simultaneous application of PLIF and PIV/PTV (Zadrazil and Markides 2014, Zadrazil, Matar and Markides 2014, Charogiannis, An and Markides 2015), we seek to extend our understanding of the phenomenology of the formation and evolution of thermal features on the film free-surface and to investigate the coupling between these thermal features and the hydrodynamic characteristics of heated falling-films, by simultaneously conducting thermography and velocimetry measurements on the gas-liquid interface (Kabov, Scheid, Sharina and Legros 2002). The proposed experimental technique aims to achieve this by employing highly reflective, silver-coated particles, which when suspended near or at the gas-liquid interface, are imaged as highly-localized thermal radiation peaks or troughs due to their differing emissivity characteristics compared to the surrounding fluid. It should be noted that despite the fact that the development of this technique, which we refer to as "thermographic particle velocimetry" (TPV), builds upon our previous work on heated falling-films and is intended for such studies, the same measurement principle can also be applied for the recovery of 2-D temperature- and velocity-field information at the common interface of any flow with a significant density gradient between the two phases. Thus, the applicability of TPV extends to numerous multiphase/interfacial-flow investigations where detailed measurements are currently performed by employment of laser techniques.

As we noted above, TPV relies on the use of highly reflective, silver-coated particles, which when suspended near or at the air–liquid interface, are imaged as highly localized thermal radiation peaks or troughs. The thermal radiation collected by an IR detector, I_{meas}, when the latter is positioned above the liquid interface follows Eq. (1):

$$I_{\mathrm{meas}} = \epsilon I_{\mathrm{li}} - (1-\epsilon) I_{\mathrm{bg}}, \quad (1)$$

where I_{li} stands for the thermal radiation emitted by the liquid, ϵ for the emissivity of the liquid free-surface, and I_{bg} for the background radiation reflected by the liquid surface due to its reflectivity $\rho = 1 - \epsilon$. The emissivity of liquids that are commonly employed in film-flow investigations, such as water and glycerol (which we also employ in our experiments),

corresponds to ≈ 0.96 (Brewster 1992); in contrast, the emissivity of silver is below 0.1, even when oxidized. Thus, for particles which reflect strongly the background radiation, the emissive power collected by the IR thermograph will be largely dependent on the background/ambient temperature. Based on this thesis, there are two ways by which reflective particles appear distinct from the neighboring fluid: (i) if the background temperature exceeds the flow temperature the particles appear as local "hot-spots", or (ii) if the flow temperature exceeds the background temperature they appear as local "dark-spots". In Fig. 1, we present raw IR images that are illustrative of both scenarios.

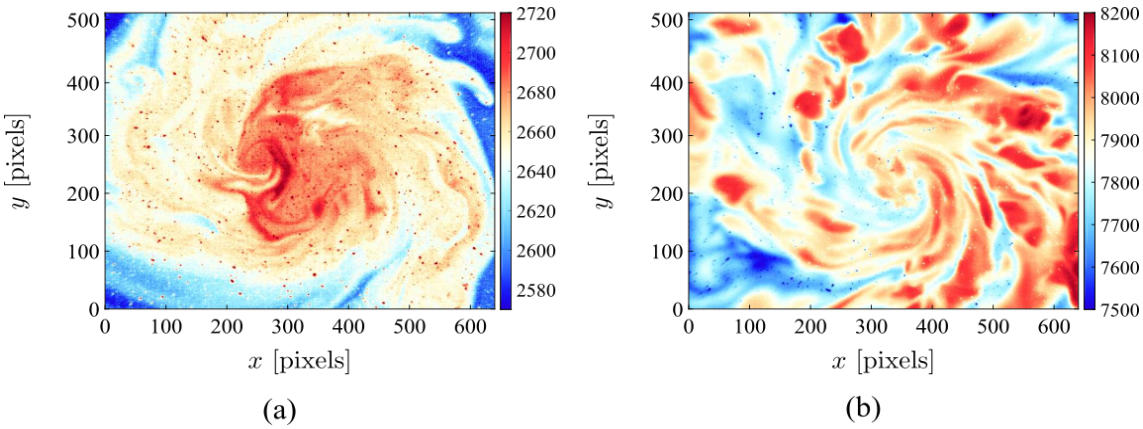

Fig. 1 Raw IR images of particle-laden, heated and stirred flows of water inside an open container. (a) Images collected while the water temperature (≈ 10 °C) is lower than the room temperature (≈ 25 °C), and (b) images collected while the water temperature (≈ 50 °C) is higher than the ambient. This figure is reproduced from Ref. (Charogiannis, Zadrazil and Markides 2016).

Another crucial aspect associated with the proposed measurement technique and in particular its applicability in film-flows as well as any other multiphase/interfacial flow study, is concerned with the transmittance characteristics of the employed fluid over the effective spectral band of the IR thermograph; if the employed liquid is highly transmissive, the temperature measurement produced by an IR thermograph set up atop of the fluid flow will correspond to a bulk-averaged temperature measurement, rather than an interfacial temperature measurement. Even though some of the commonly employed liquids in interfacial flow investigations, such as water and glycerol, are effectively opaque over broad IR spectral bands (see, for example, Fig. 2 (b)), thus allowing for temperature measurements that are intergraded over extremely shallow optical depths, knowledge of the transmittance characteristics of these fluids can prove particularly beneficial when seeking to employ TPV in a two-phase flows comprising two immiscible liquids. For example, our ATR (attenuated total reflectance) spectral measurements

reveal a wide, low-transmittance band that is common to both water and glycerol. This band is not, however, shared with common oils. Thus, the use of appropriate IR filters would allow, in this case, TPV measurements in two-phase flows comprising the particular liquids.

3. Experimental setup

In developing the experimental methodology and associated image-processing steps, a simple experimental arrangement was employed (see Fig. 3). A cooled, mid-wave FLIR X6540sc camera (640 × 520 pixel detector, 15 μm pitch, thermal sensitivity of ≈ 18 mK and maximum recording frequency of 126 Hz at full resolution) was positioned atop a heated and stirred flow of water inside an open container, seeded with silver-coated glass particles (glass hollow spheres, 100 μm average diameter, 12% silver content by weight, 0.9 g/cc density) purchased from Hart Materials Ltd. The particles were selected to be buoyant/neutral in order to allow for interfacial velocity measurements with only modest seeding concentrations. The camera was equipped with a 25 mm, F/2 lens (transmissivity over the range 2.5 − 5 μm), allowing for a maximum spatial resolution of up to ≈ 100 μm/pixel, while the image integration-time was set to 843 μs. The flow was generated using a 650 W IKA RCT magnetic stirrer with intergraded temperature control.

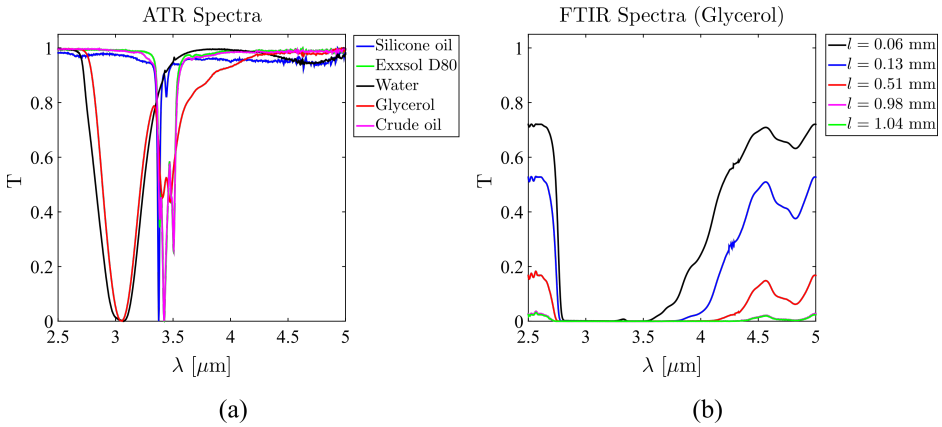

(a) (b)

Fig. 2 (a) ATR (attenuated total reflectance) spectra of commonly employed liquids in film-flow investigations and (b) FTIR (Fourier-transform infrared) spectra of glycerol as a function of sample thickness (i.e. IR radiation path-length), measured over the effective spectral range of our IR thermograph (2.5—5 μm).

In these experiments, the camera was positioned at a distance of ≈ 20 cm from the liquid surface, while the camera axis was set up at an angle of approximately 20 ° to the flow in order to prevent it from capturing an image of itself. Consequently, perspective distortion corrections were implemented later on during processing using a thermal-target image of known spatial coordinates.

The target itself comprises a black carton background and a perforated steel-sheet (4.7 × 4.7 mm rectangular holes, 8 mm pitch). The latter was polished in order to increase its reflectivity, and thus, the contrast with the black-carton background. A raw thermal image of the target is presented in Fig. 4, alongside its perspective-distortion corrected counterpart. The correction was performed in LaVision Davis by employment of a camera pinhole-model. Based on the optics that was installed on the IR camera, a maximum spatial resolution of up to ≈ 100 μm/pixel was achieved.

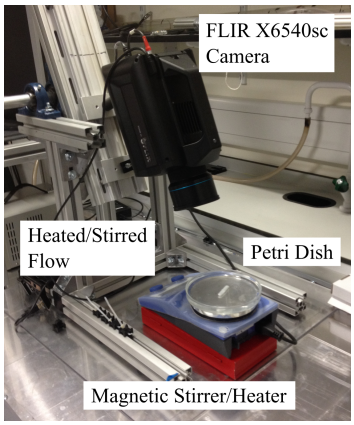

Fig. 3 Photograph of the experimental setup used for developing the imaging technique and relevant image-processing steps. Reproduced from Ref. (Charogiannis, Zadrazil and Markides 2016).

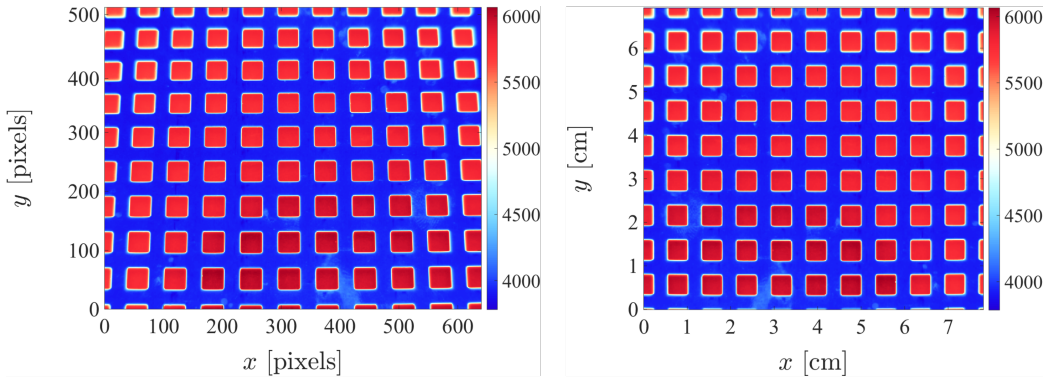

(a) (b)

Fig. 4 (a) Raw IR image of the thermal target used in order to correct the collected image sequences for perspective distortions. (b) The same image following the perspective-distortion correction performed in LaVision Davis.

Once a set of raw thermal images is collected and corrected for the non-unity emissivity of the liquid using the IR-camera software provided by FLIR (ResearchIR 4), it is imported in Matlab and processed using an algorithm that was developed in-house. Firstly, the particles are identified by subtracting a moving average (3 × 3 window), and two separate frames are

generated; one containing only the particles, and a second thermal image of the flow with the particles removed (see Fig. 5). The former are also subjected to a threshold intensity-level, determined *a priori* by conducting experiments without particles in the flow, in order to remove any noise and minimize any inaccuracies in the PIV calculation. Rather than using a fixed threshold-level, a function that links the noise level to the liquid temperature is generated, and fitted using a power-law curve (see Fig. 6). Once the particle-only frame is fully processed, it is used to mask out the pixels corresponding to particles in the thermal frame, which is then reconstructed by substituting those values with the average of their neighbors. Both thermal and particle frames are then imported in LaVision Davis and corrected for perspective distortions (the resulting apparent resolution corresponds to 110 μm/pixel in these experiments). The perspective-distortion corrected thermal frames are finally imported back into MATLAB, and converted to 2-D temperature maps using the IR-camera calibration curve (see Fig. 7), that links the thermal radiation collected from a blackbody to the blackbody temperature.

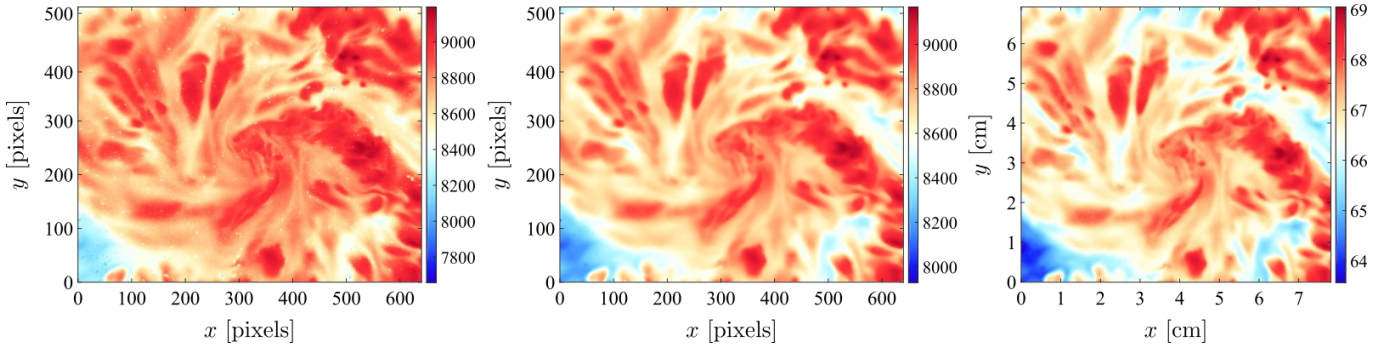

Fig. 5 (a) Raw thermal image of the particle-laden, heated and stirred water-flow; colour-scale indicates the intensity of the collected thermal radiation. (b) The same image following removal of the reflective particles. (c) Interfacial temperature measurement performed using the camera calibration-curve (Fig. 7). Reproduced from Ref. (Charogiannis, Zadrazil and Markides 2016).

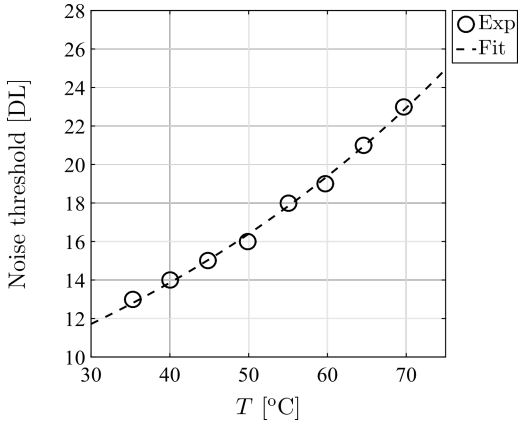

Fig. 6 Noise-threshold function employed in order to increase the signal-to-noise ratio of the particle-only images, and improve the accuracy of the PIV calculation.

The particle frames are processed using a four-pass cross-correlation with a 64 × 64 pixel interrogation window and 50% overlap for the first two passes, and a 32 × 32 pixel window in the final two passes, resulting in a 1.7 mm vector-to-vector spatial resolution. Additional processing steps are applied to the velocity-vector maps that were generated during the first three passes, and include the use of a cross-correlation detectability filter that rejects particle-group displacements that display low cross-correlation values, median filtering for removing any spurious vectors, a vector density filter coupled with interpolation/extrapolation in the empty regions, and a finally, a 3 × 3 smoothing filter. Individual particles are also tracked (PTV calculation), using the PIV results as reference estimators of the 2-D velocity distribution. A 1 × 3 pixel allowable particle-size range is applied, with a 4 × 4 pixel window for particle correlation and a ± 2 pixel allowable vector-range relative to the reference velocity (PIV result). The PIV and PTV velocity-vector maps obtained from images such as Fig. 8 (c) are overlaid with the temperature field (Fig. 5(c)) and are presented in Fig. 9 (b) and (c). Finally, 100-image average temperature and velocity maps are presented in Fig. 10 for different liquid temperatures.

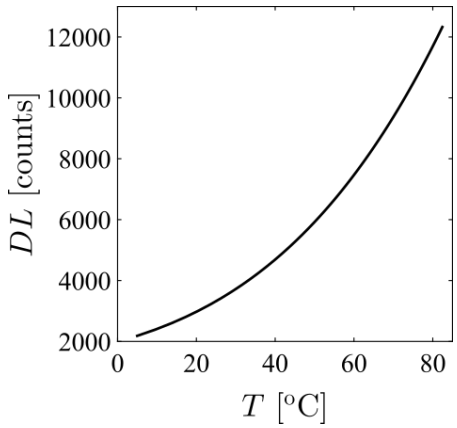

Fig. 7 IR camera calibration curve that links the collected thermal radiation level to the temperature of a blackbody, for a frame-integration time of 843 μs.

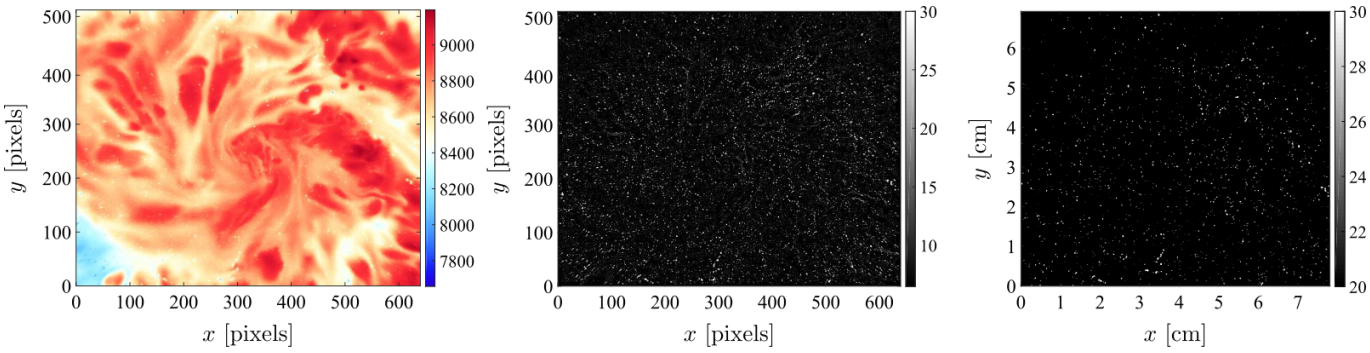

Fig. 8 (a) Raw thermal image of the particle-laden, heated and stirred water-flow. (b) Particle image generated by applying a moving-average subtraction to the raw image. (c) The same image following noise removal. Reproduced from Ref. (Charogiannis, Zadrazil and Markides 2016).

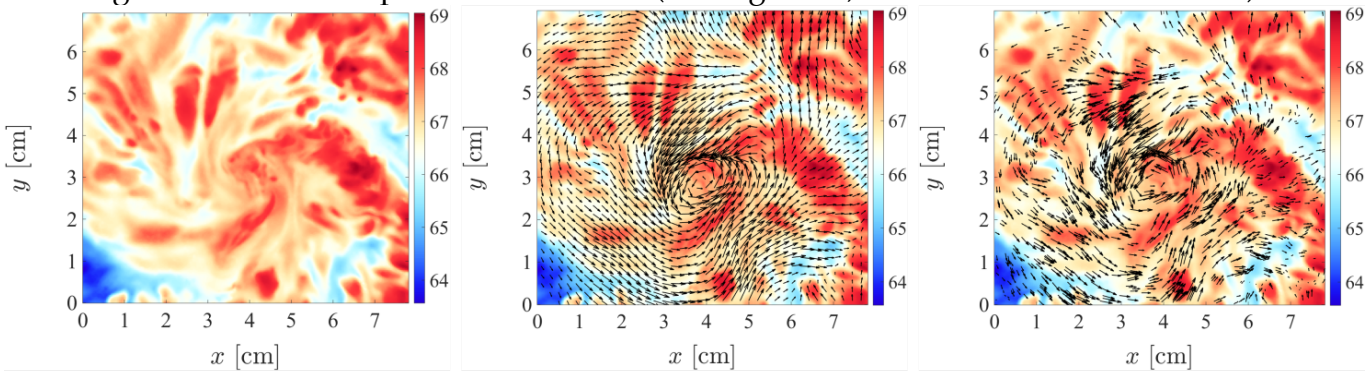

Fig. 9 (a) Interfacial temperature measurement generated from the IR image of Fig. 5 (c). (b) Combined temperature and velocity-vector map of the flow-interface, generated using PIV. (c) Combined temperature and velocity-vector map of the flow-interface generated using PTV. Reproduced from Ref. (Charogiannis, Zadrazil and Markides 2016).

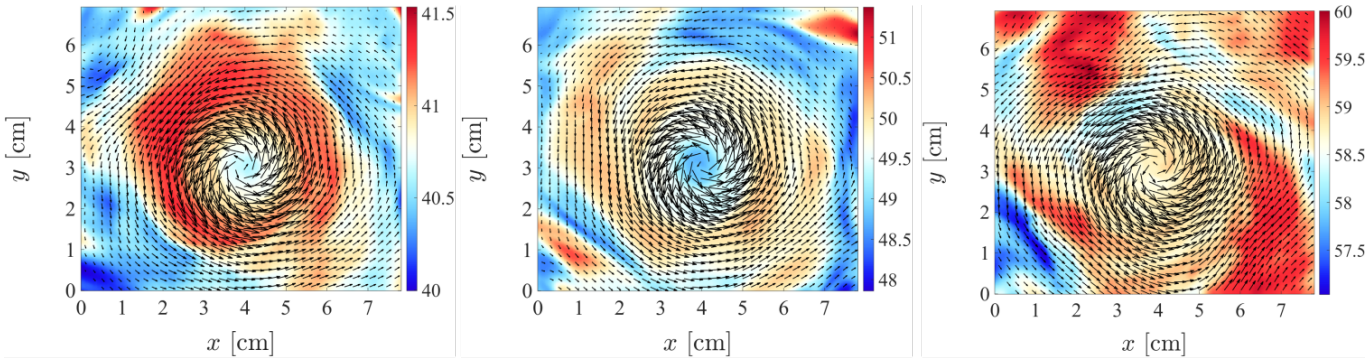

Fig. 10 Time-averaged temperature and velocity measurements of heated and stirred water-flows. The mean interfacial temperatures correspond to (a) ≈ 41 °C, (b) 50 °C, and (c) 59 °C.

4. Results and discussion

4.1 Validation experiments: Temperature-measurement validation

Having developed and optimized the processing routines using the simple setup described earlier, temperature- and velocity-validation experiments were performed, the former using the same setup, and the latter by employment of the falling-film apparatus described in Ref. (Charogiannis, An and Markides 2015). In first case, temperature measurements were recorded with the IR camera and pre-calibrated K-type thermocouples (the thermocouple arrangement is shown in Fig. 11 (a)), while the liquid was cooling down from approximately 80 °C, with the heater switched off and the flow continuously stirred. Time-averaged, 2-D temperature maps of the liquid surface collected at different instances during the cooling process are presented in Fig. 11. Also shown in Fig. 11 (a), are the four regions of interest (ROIs) from which IR temperature data were extracted and compared to the thermocouple measurements.

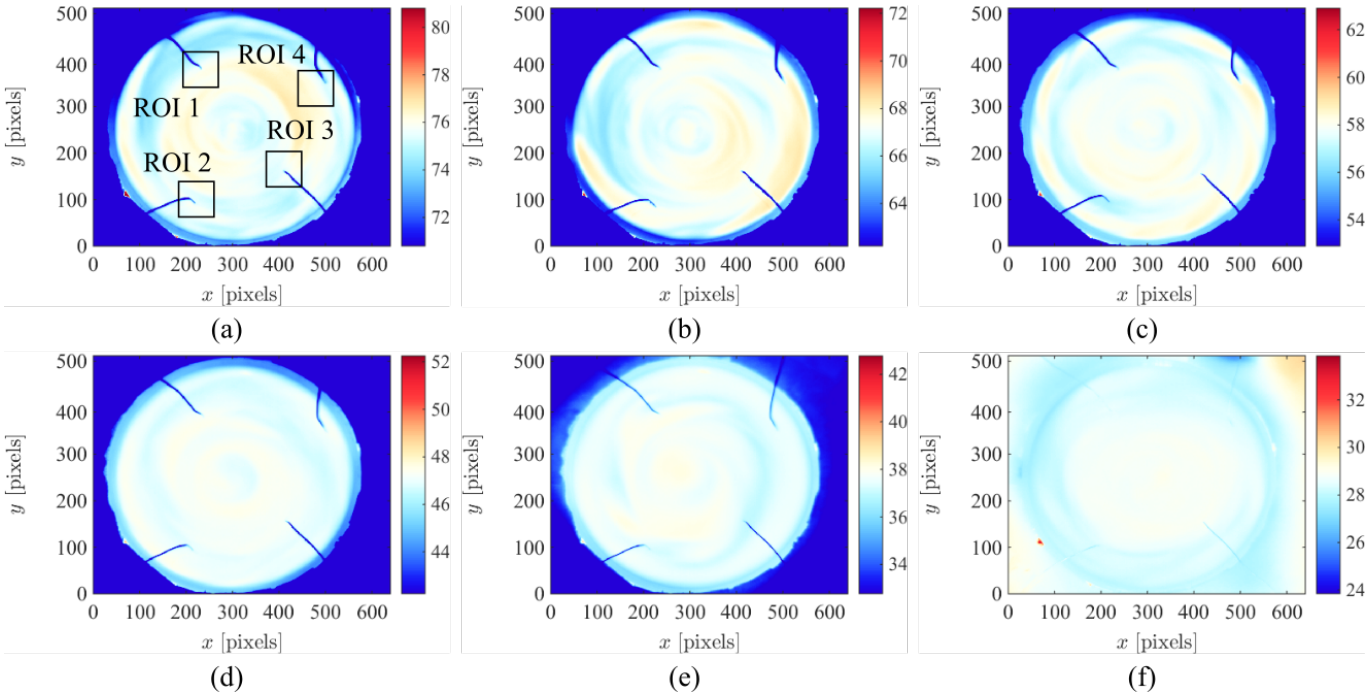

Fig. 11 (a) Time-averaged temperature distribution of the liquid surface. The thermocouple arrangement and ROIs used for further processing are also indicated. (b) - (f) Time-averaged temperature distributions of the liquid surface collected at later stages of the cooling down process.

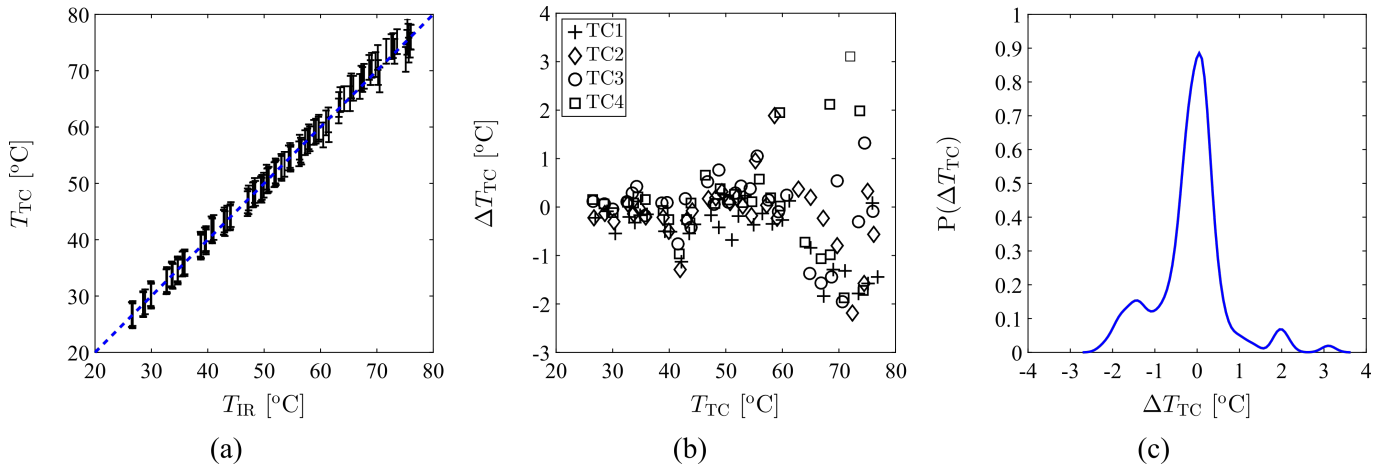

Fig. 12 (a) Temperature measurements, T_{IR}, conducted using the IR camera and plotted against thermocouple measurements, T_{TC}, over the range 25 – 80 °C. (b) Temperature measurement deviation, ΔT_{TC}, between the thermocouple and IR camera measurements, plotted against the latter. (c) PDF of ΔT_{TC}, compiled using the data plotted in (a). Subfigures 12 (a) and (c) are reproduced from Ref. (Charogiannis, Zadrazil and Markides 2016).

Once the experiment was completed, the temperature measurements of each ROI were averaged, and the results were plotted against their corresponding thermocouple measurements (Fig 12 (a)). The deviation between the IR camera and thermocouple results over the examined temperature range (25—80 °C) is below ± 0.5 °C at a 64% confidence level, and below ± 1 °C at an 80% confidence level. The largest deviations are encountered over the first few measurements (high-temperature measurements), most probably owing to stronger temperature inhomogeneities within the flow.

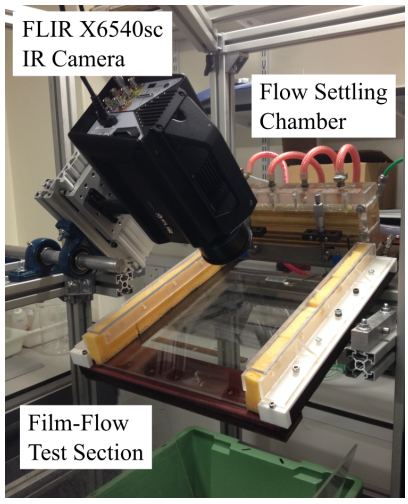

Fig. 13 Photograph of the experimental facility used in the velocity validation and localized-heating experiments, the latter performed for demonstrating the technique capabilities in a practical film-flow investigation. Reproduced from Ref. (Charogiannis, Zadrazil and Markides 2016).

4.2 Validation experiments: Velocity-measurement validation

The validity of the proposed interfacial-velocity measurement was assessed by conducting tests in our falling-film facility, comprising a planar test-section over which liquid-film flows develop, a settling chamber installed at the test-section inlet, and a closed flow-loop that incorporates a pump and a heat exchanger (Fig. 13). In the absence of interfacial waves, the velocity profile across the liquid film can be obtained analytically using the 1-D, steady, fully developed solution of the Navier-Stokes equation for a gravity-driven flow, also referred to as the Nusselt solution (Eq. 2). In order to approximate the flow condition described by the Nusselt solution, the growth of interfacial waves is moderated in the experiment by selecting a high glycerol content (approximately 80% glycerol by weight), and therefore a highly viscous, aqueous-glycerol solution, which allows the film to remain flat over an extended spatial domain (i.e., a long distance from the inlet). The velocity at the interface, U_{Nu}, is given by:

$$U_{\mathrm{Nu}} = \frac{1}{2}\left(\frac{g\sin\beta}{v_{\mathrm{f}}}\right)^{1/3}\left(\frac{3Q}{w}\right)^{2/3}, \quad (2)$$

where β stands for the substrate inclination angle (30 °), v_f for the liquid kinematic viscosity, Q for the liquid flow-rate, and w for the liquid-film span (290 mm). In order to obtain different values of U_{Nu}, the flow Reynolds number (Re) was varied in the range $Re = 0.6 - 11.8$ by varying the liquid flow-rate between $Q = 0.11\times10^{-4}$ and 1.28×10^{-4} m^3/s. The kinematic viscosity was also varied in the range $v_f = 3.75\times10^{-4} - 6.42\times10^{-4}$ m^2/s by adjusting the liquid temperature between 19.3 °C and 28.3 °C. Using the liquid temperature measurements and the known water/glycerol concentrations, the kinematic viscosity was determined by employment of the parameterization provided by Cheng (Cheng 2015). The resulting range of U_{Nu} values corresponds to $U_{\mathrm{Nu}} = 0.05 - 0.31$ m/s.

As these TPV measurements were performed under isothermal (room temperature) conditions, it was necessary to illuminate the silver-coated particles in order to increase the contrast with which they appear on the thermal images relative to the surrounding liquid. Towards that end, a 150 W IR heater was installed next to the test section. Thermocouple measurements were carried out in order to assess the effect of radiative heating on the film-flow over a range of flow rates while the heater was operated, with the resulting temperature difference between runs with the heater on and off being approximately 1 °C for $Re < 0.8$. This result suggests that the employed illumination practice does not affect the flow or liquid properties.

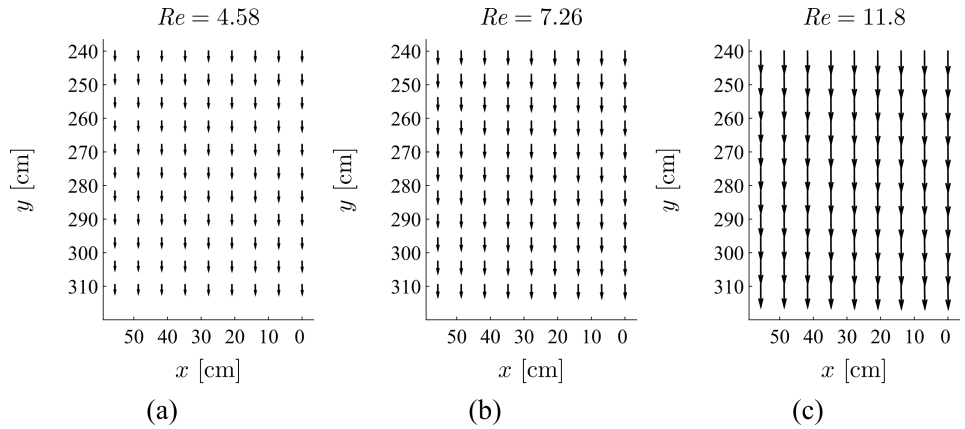

Fig. 14 Interfacial velocity distributions of viscous film-flows pertaining to (a) $Re = 4.58$, (b) 7.26 and (c) 11.8. The x-axis represents the distance along the film span, measured from the flow centerline. Subfigure 14 (c) is reproduced from Ref. (Charogiannis, Zadrazil and Markides 2016).

The results of our validation experiments are presented in Fig. 15, while typical PIV vector-maps are presented in Fig. 14. It should be noted that for these experiments, a two-pass cross-correlation with the interrogation window and overlap set to 128 × 128 pixels and 50%, respectively, were employed as the investigated flows involve only small spanwise gradients. The mean deviation between the experimentally-derived interfacial velocities and the analytically calculated ones based on the Nusselt solution was ≈ 2% over the range 0.05 − 0.3 m/s . The error bars in Fig. 15 indicate the error associated with the analytical calculations (around 4%), which stems mainly from the flow rate, density and viscosity measurements. Finally, we would like to emphasize that this experiment also demonstrates the prospective employment of the proposed technique in isothermal film-flows, whereby interfacial velocities can be recovered over an extended spatial domain with little experimental effort.

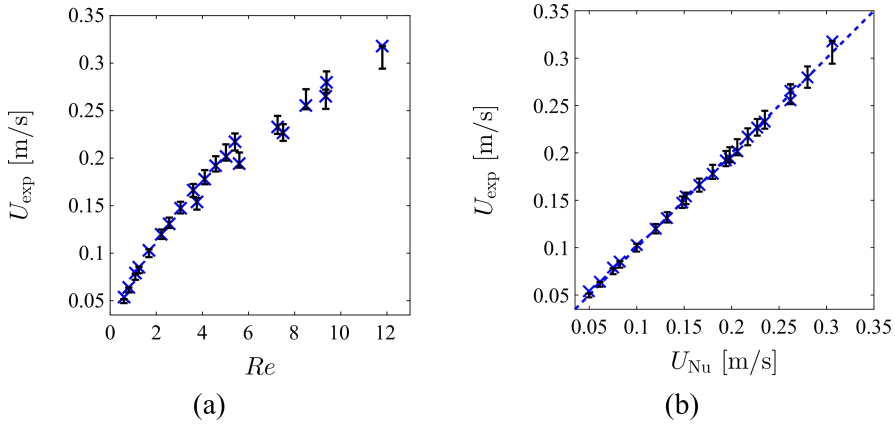

Fig. 15 Interfacial velocity measurements U_{exp}, extracted from TPV-derived interfacial-velocity maps such as those presented in Fig. 14, and plotted against (a) the flow Re, and (b) the analytically calculated interfacial-velocity values pertaining to the same flow conditions, U_{Nu}. Subfigure 15 (b) is reproduced from Ref. (Charogiannis, Zadrazil and Markides 2016).

4.3 Film-flow experiments

For the purposes of this experiment, the glass substrate of the film-flow facility was replaced by a Perspex plate with a 4 × 1.2 mm groove cut across the direction of the flow along the test-section centerline, at a distance of 7.5 cm from the flow inlet. A rectangular steel-sleeve with a 200 W cartridge heater was inserted in the groove, and powered by a programmable 6 kW power supply purchased from Magna-Power Electronics Ltd. Deionized water at 17.5 °C was used instead of the viscous water-glycerol solution employed in the previous runs, while the substrate inclination angle was reduced to 15 °. Finally, the power input to the cartridge heater was set to 44 W (the resulting heat flux into the liquid being 8.4 W/cm^2).

Thermal images were recorded between $y = 4.5 - 9$ cm downstream of the heater, for flows pertaining to $Re = 80$, 100 and 120. The images were processed according to the procedures described earlier, and the resulting particle-image sequences were processed using a four-pass cross-correlation, with the final window size set to 48 × 48 pixels and the overlap to 50%. The corresponding vector-to-vector resolution is 2.6 mm. Fully-processed sample images of the temperature and velocity fields are presented in Fig. 16, revealing complex thermal features and a highly inhomogeneous velocity distribution. Owing to the high *Re* values selected for this experiment, it is believed that the observed velocity-field non-uniformities and strong waviness are driven by inertia and gravity, rather than the thermocapillary (Marangoni) instability.

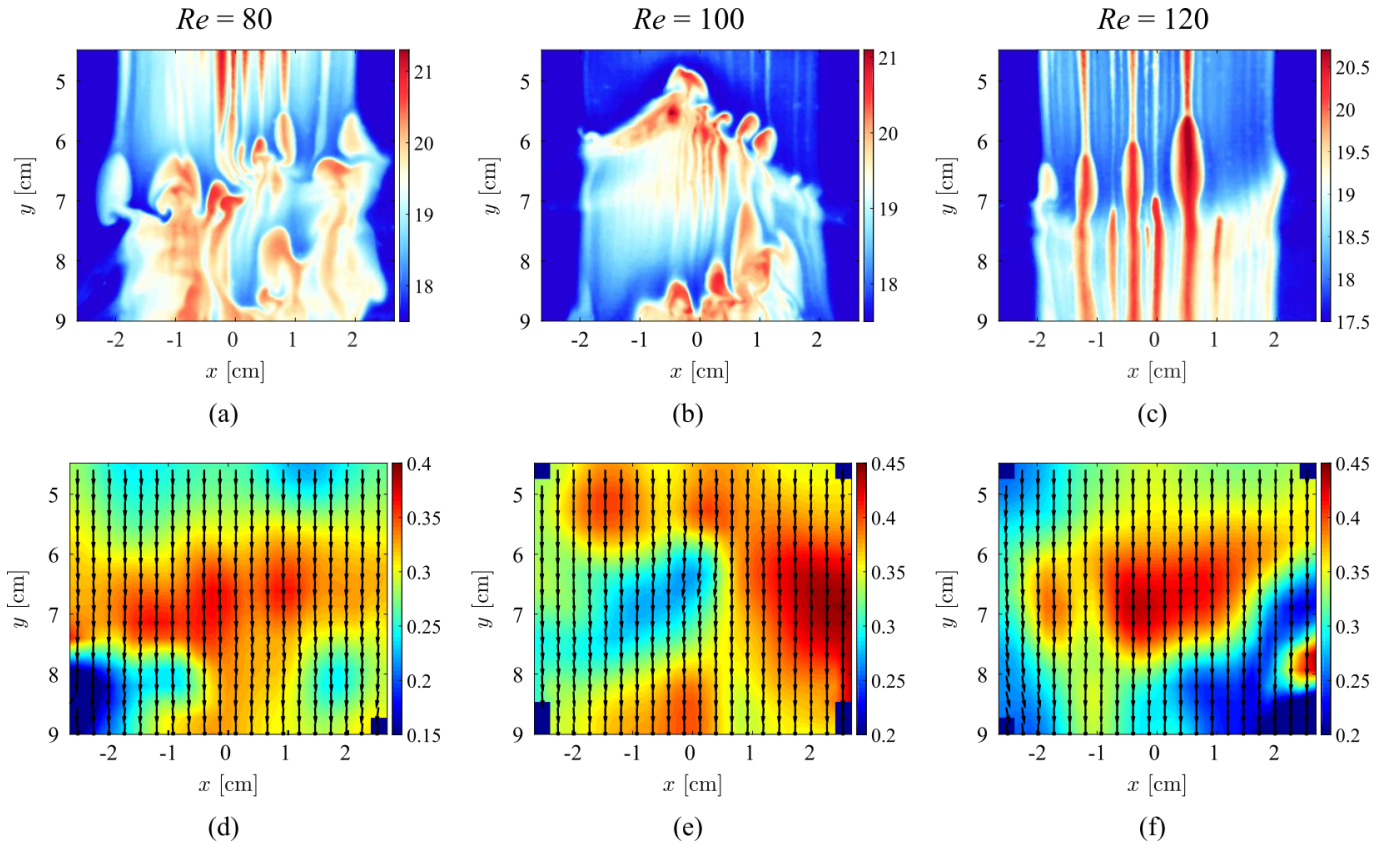

Fig. 17 Simultaneously measured temperature and velocity distributions at the gas-liquid interface of locally heated falling-films ($Re = 80, 100, 120$). The y-axis indicates the distance of the imaging region from the cartridge heater, while the colour-scales indicate the magnitude of the local temperature and velocity in °C and m/s. The arrows in the PIV maps indicate the flow direction.

5. Conclusions

The development and validation of a combined thermographic velocimetry technique was presented in this contribution, followed by its application in a locally-heated falling-film flow. The technique, which we refer to as thermographic particle velocimetry (TPV), employs a single IR imager and highly-reflective particles in order to simultaneously recover the temperature and velocity distributions at the common interface of multiphase flows, and thus, constitutes an easy to implement diagnostic tool for the study of either isothermal or non-isothermal interfacial flows. Given the presence of a sufficient density gradient between the two phases, the applicability of TPV extends to numerous multiphase/interfacial-flow investigations where detailed measurements are currently performed by employment of laser techniques.

The image processing steps used to retrieve temperature and velocity information were demonstrated by application of the proposed TPV methodology in a heated and stirred flow in

an open container. These include the decomposition of raw IR frames into separate thermal and particle frames, the application of perspective distortion corrections, spatial calibration, and filtering operations, and finally the use of standard PIV algorithms. In addition, two validation experiments were also conducted and presented, indicating that the deviations between any results generated by TPV and those stemming from conventional methods do not exceed the errors encountered in the latter. Finally, TPV was applied in the investigation of the interfacial characteristics of locally-heated falling-film flows, revealing the presence of complex thermal structures and highly inhomogeneous flow-fields, with high spatial and temporal resolution.

Acknowledgements

This work was supported by the UK Engineering and Physical Sciences Research Council (EPSRC) [grant numbers EP/K008595/1 and EP/L020564/1].

List of references

Alekseenko SV, Nakoryakov VY, Pokusaev BG (1985). Wave formation on a vertical falling liquid film. AIChE J 31: 1446-1460.
Brewster MQ (1992). Thermal Radiative Transfer and Properties, Wiley-Interscience.
Charogiannis A, An JS, Markides CN (2015). A simultaneous planar laser-induced fluorescence, particle image velocimetry and particle tracking velocimetry technique for the investigation of thin liquid-film flows. Exp Therm Fluid Sci 68: 516-536.
Charogiannis A, Zadrazil I, Markides CN (2016). Thermographic particle velocimetry (TPV) for simultaneous interfacial temperature and velocity measurements. Int J Heat Mass Transfer 97: 589-595.
Cheng N-S (2015). Formula for the viscosity of a glycerol-water mixture. Ind Eng Chem Res 47: 3285-3288.
Chinnov EA, Abdurakipov SS (2013). Thermal entry length in falling liquid films at high reynolds numbers. Int J Heat Mass Transfer 56: 775-786.
Chinnov EA, Kabov OA (2007). Marangoni effect on wave structure in liquid films. Microgravity Sci Technol 19: 18-22.
Chinnov EA, Shatskii EN (2010). Effect of thermocapillary perturbations on the wave motion in heated falling liquid film. Tech Phys Lett 36: 53–56.
Chinnov EA, Shatskii EN, Kabov OA (2012). Evolution of the temperature field at the three-dimensional wave front in a heated liquid film. High Temp 50: 98-105.
Kabov OA, Scheid B, Sharina IA, Legros J-C (2002). Heat transfer and rivulet structures formation in a falling thin liquid film locally heated. Int J Therm Sci 41: 664-672.
Kapitza PL (1948). Wave flow of thin layers of a viscous fluid. Z Eksp Teor Fiz 18: 3-28.

Kapitza PL, Kapitza SP (1949). Wave flow on thin layers of a viscous fluid. Z Eksp Teor Fiz 31: 105-120.
Lel VV, Kellermann A, Dietze G, Kneer R, Pavlenko AN (2008). Investigations of the marangoni effect on the regular structures in heated wavy liquid films. Exp Fluids 44: 341-354.
Markides CN, Mathie R, Charogiannis A (2015). An experimental study of spatiotemporally resolved heat transfer in thin liquid-film flows falling over an inclined heated foil. Int J Heat Mass Transfer 93: 872–888.
Mathie R, Markides CN (2013). Heat transfer augmentation in unsteady conjugate thermal systems – Part I: Semi-analytical 1–D framework. Int J Heat Mass Transfer 56: 802-818.
Mathie R, Nakamura H, Markides CN (2013). Heat transfer augmentation in unsteady conjugate thermal systems – Part II: Applications. Int J Heat Mass Transfer 56: 819-833.
Moran K, Inumaru J, Kawaji M (2002). Instantaneous hydrodynamics of a laminar wavy liquid film. Int J Multiphase Flow 28: 731-755.
Morgan RG, Markides CN, Hale CP, Hewitt GF (2012). Horizontal liquid-liquid flow characteristics at low superficial velocities using laser-induced fluorescence. Int J Multiphase Flow 43: 101-117.
Morgan RG, Markides CN, Zadrazil I, Hewitt GF (2013). Characteristics of horizontal liquid-liquid flows in a circular pipe using simultaneous high-speed laser-induced fluorescence and particle velocimetry. Int J Multiphase Flow 49: 99-118.
Peng J, Wang M-M, Geng J, Wu Y-T, Zhang Z-B (2012). Falling film of ionic liquid-water binary solutions on a uniformly heated vertical wall. J Heat Transfer 134: 0145021–0145025.
Rietz M, Rohlfs W, Kneer R, Scheid B (2015). Investigations of the marangoni effect on the regular structures in heated wavy liquid films. EPJ ST 224: 355-368.
Zadrazil I, Markides CN (2014). An experimental characterization of liquid films in downwards co-current gas-liquid annular flow by particle image and tracking velocimetry. Int J Multiphase Flow 68: 1-12.
Zadrazil I, Matar OK, Markides CN (2014). An experimental characterization of downwards gas-liquid annular flow by laser-induced fluorescence: Flow regimes and film statistics. Int J Multiphase Flow 60: 87-102.
Zhang F, Peng J, Geng J, Wang Z-X, Zhang Z-B (2009). Thermal imaging study on the surface wave of heated falling liquid films. Exp Therm Fluid Sci 33: 424-430.
Zhang F, Zhao X, Geng J, Wu Y-T, Zhang Z-B (2007). A new insight into marangoni effect in non-isothermal falling liquid films. Exp Therm Fluid Sci 31: 361-365.